

Final design of the cryostat for the high luminosity LHC magnets

D Ramos, A Vande Craen, H Prin, Y Leclercq, L Williams, M Struik, G Barlow, O Riu Martinez, B Wong Luis, V Parma, F Savary and E Todesco

CERN, CH-1211 Geneva 23, Switzerland

Email: Delio.Ramos@cern.ch

Abstract. The high luminosity LHC project (HL-LHC) aims at increasing proton collisions by a factor of ten whilst extending physics exploitation until 2035. Its performance will rely on new focusing quadrupoles, beam separation dipoles and corrector magnets with large apertures to be installed on both sides of the ATLAS and CMS experiments. A dedicated cryostat design of about 1 m in diameter was developed for operation of these magnets at 1.9 K, comprising the required cryogenic circuits, interconnects, supports, insulation, and instrumentation systems.

Six cryostats with various lengths in the range of 8 to 11 m are required on each side of the interaction points to house the triplet magnets, correctors and the first separation dipole. These cryostats will be linked through flexible interconnects to form a continuous vacuum insulation and cryogenic system of about 60 m in length. The second rearmost separation dipole requires a stand-alone cryostat of 15 m in length but nevertheless features common design principles.

We present the design of these cryostats, from a conceptual stage towards the final design. Assembly aspects are also addressed, including a modular approach affording flexibility and simplification of the manufacturing and assembly processes.

1. Introduction

The Large Hadron Collider (LHC) is a 27 km circumference particle accelerator based on superconducting Nb-Ti magnets operating in superfluid helium at 1.9 K. It has been colliding proton and heavy ion beams since it was successfully commissioned in 2010. The high luminosity LHC (HL-LHC) is an on-going project aiming to upgrade the LHC accelerator and extend its discovery potential [1]. The upgrade will rely on new superconducting magnets to be installed on both sides of the ATLAS and CMS experiments [2]. Enlarged magnet aperture and high peak field are achieved by switching from Nb-Ti to Nb₃Sn superconductor technology in the three quadrupoles closest to the interaction points (Q1-Q2-Q3, also known as triplet). The upgrade also includes the replacement of the beam separation and recombination dipoles with new Nb-Ti magnets. Magnet operation will remain at 1.9 K, but new refrigerators will be installed to cope with the increased heat loads induced by collision debris.

A new cryostat design is required, imposed by additional constraints resulting from a very compact integration environment, significantly higher dynamic heat loads and the need for accurate magnet positioning throughout the operational lifetime. Hereafter we review the layout, the main design choices introduced since the conceptual design [3] and further detail the solutions implemented in the final design of the cryostats for the HL-LHC magnets.



2. Layout of the interaction region magnets and cryostats

The HL-LHC interaction region magnets are assembled into five different types of cold masses: two types for the triplet cold masses (Q1/Q3 and Q2), one type for the separation dipole D1, one type for the recombination dipole D2 and a fifth type grouping an orbit corrector, skew quadrupole corrector and several high order correctors. The latter, named a corrector package (CP), is located between Q3 and D1. Each cold mass is first individually assembled into its specific cryostat to form a cryo-magnet. The six cryo-magnets comprising the triplet, CP and D1 are then interconnected in the tunnel to form a continuous cryostat of approximately 60 m in length, spanning from about 20 to 80 m distance from the interaction points (see figure 1). The D2 cold mass sits in a stand-alone cryostat at about 140 m from the interaction point. Individual cryostats vary between 8 and 15 m in length, with weights in the range of 16 to 30 tonne.

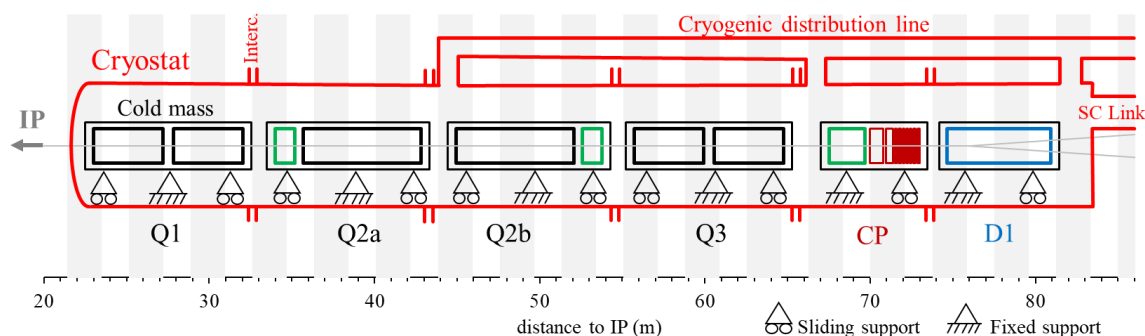


Figure 1. Final layout of the continuous cryostat comprising the triplet (Q1, Q2a/b, Q3), the corrector package (CP) and the separation dipole D1.

Given the heat load profile, cooling of the Q1 to D1 string of cold masses is best achieved through linear heat exchangers, as in the existing LHC magnets, where saturated superfluid liquid helium flows downwards with the tunnel slope [4]. However, the application of such a solution in the tunnel sections close to the experiments imposes the integration of some cryogenic lines inside the magnet cryostat itself, as opposed to a completely external line supplying the LHC arcs. This is because of the radiation shielding reducing the tunnel diameter towards each of the interaction points. Given the total heat load, of the order of 1400 W over the 60 m length and the limited diameter of the heat exchanger tubes, a diameter imposed by the magnet design, the heat exchangers were finally split into three independent pipe runs. Each heat exchanger run provides cooling for two of the six consecutive cold masses. By placing the first connection to the cryogenic distribution line (jumper) in the interconnection between the two Q2 cold masses, it was possible to comply with the locally reduced diameter of the tunnel in the Q1 region. Such a layout with cryogenic lines running inside the vacuum vessel became a determinant factor in the design of the whole cryostat, including the cold mass supports and the positioning of the various elements in the cross-section.

In contrast, cooling of the D2 cold mass is achieved with a localised heat exchanger installed on one extremity of the cold mass [5]. The major advantages of such heat exchanger are that its performance is independent from the tunnel slope and the heat exchanger dimensions are decoupled from the magnet design. A D2 cryostat cross-section similar to that of Q1 to D1 was nevertheless adopted for reasons of standardisation of components, and especially of the assembly tooling.

3. Key design features

The final cross-section of the cryostat is presented in figure 2. From the conceptual design phase, it became evident that a cryostat design based on a cold mass supported on columns, as adopted in the LHC arcs [6], was the most suitable solution for the new interaction regions. A support scheme consisting of two to three columns, depending on the cold mass length and maximum allowable sagitta, could be designed to provide the required strength and stability with acceptable performance in terms

of heat loads. Moreover, there was the experience with fabrication and assembly of the LHC cryostats to capitalise on, as well as the positive feedback coming from a decade of exploitation.

One of the challenges was to integrate the cold mass, its supports, an actively cooled thermal shield, and various cryogenic and auxiliary busbar lines, into a cross section that was limited to a maximum of one meter in width due to transport constraints in the LHC tunnel. This requires installing a cold mass that is 70 mm larger in diameter than an LHC dipole cold mass, plus additional piping up to 100 mm in diameter, into a vacuum vessel that cannot differ much in size from that of the LHC. A vacuum vessel of elliptical or oval shape was briefly considered but then abandoned due to higher manufacturing costs and a potentially less reliable insulation vacuum sealing.

The final design consists of a cold mass axis located 54 mm below the axis of a cylindrical vacuum vessel to make room for the cryogenic and auxiliary busbar lines located above the cold mass. To allow such an arrangement, the cold mass supports must protrude below the vacuum vessel cylinder to stand on cradles welded to reinforcement rings.

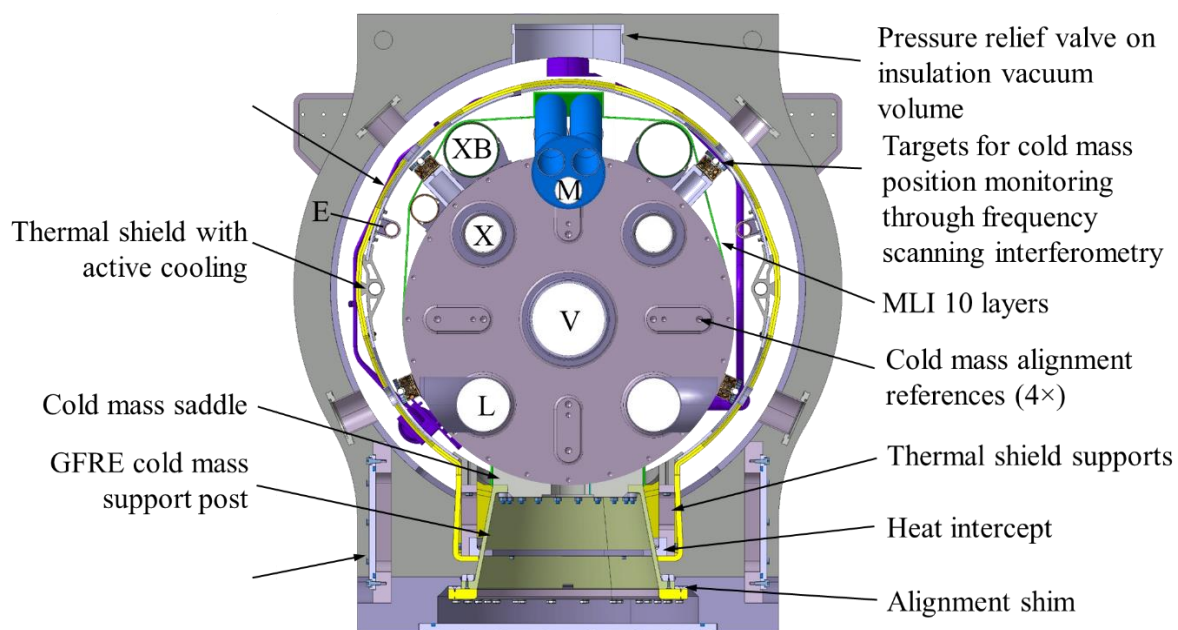


Figure 2. Cross-section of the final cryostat. The cryostat integrates cryogenic process lines for three He circuits: 1) Saturated 1.9 K liquid He heat exchanger lines (X) inside the cold mass complemented with external lines located above the cold mass (XB) for gas pumping; 2) He gas supply lines (E) at 60-80 K for thermal shield cooling; and 3) Busbar (M) and cold mass lines (L) as part of the 1.9 K pressurised He bath cooling the magnet coils.

For most LHC magnets it is enough to measure the position of the cold mass, at room temperature, with respect to fiducials installed on the outside of the vacuum vessel and to use this information to infer the magnet position once installed and at operating temperature. In the HL-LHC triplets it is important to know the magnet position with better accuracy. To remove the effects of movements during handling and transport or variations in thermal displacements, an absolute cold mass measurement system is integrated into the triplet cryostats [7]. The position of reference targets placed directly on the cold mass shell is measured by frequency scanning interferometry with optical heads installed on specific ports on the vacuum vessel.

With the smaller HL-LHC beam size at the interaction point, concerns were raised regarding eventual luminosity losses due to vibrations induced from background excitation through the tunnel floor. This led to a campaign of simulations and measurements to assess the response of the HL-LHC cryo-magnets to base excitations. Power spectral density plots for the locations concerned in the tunnel were produced

and used as input excitation to estimate the resulting vibration amplitudes at the magnet level. As any mechanical structure, a cryo-magnet assembly has resonance frequencies and therefore it was important to ensure that any amplification of vibrations, expected at such frequencies, would not influence the beam to the point of degrading peak luminosity. One may remark that a cryostat design based on a cold mass standing on column supports, inside a vacuum vessel that is itself standing on jacks, is comparable to an inverted pendulum for transverse horizontal motion. A convenient design in terms of static vertical loads and thermal management, but not optimal if subjected to horizontal mechanical excitation. Mitigation measures included increasing the distance between the two floor jacks for higher stiffness against roll angular motion; and a stiffer cold mass support as detailed in § 5.1. These measures are expected to minimise magnet vibrations, given the frequency response functions obtained by simulations of the final cryostat design and measurements on existing LHC cryo-magnets. Measurements on actual HL-LHC cryo-magnets are planned to validate the simulations and demonstrate the peak luminosity goal will not be impacted.

4. Modular design and assembly

The 28 cryo-magnets for installation in the tunnel require 19 variants to account for the specificities of each installation slot. A modular design was therefore implemented to lower procurement and assembly costs. Each cryostat was split into a standard section and a cryogenic and technical service module, as shown in figure 3. The standard section is composed of the cold mass standing on its supports inside the vacuum vessel, the thermal shield, MLI, magnet and cold mass instrumentation feeders [8] and cold mass position monitoring devices. As such, the standard section incorporates all the alignment related features and magnet diagnostics, but its design is not slope dependent nor limited to a specific insertion slot in the LHC. Only six variants of standard section are needed: one variant for Q1 and Q3, plus one for each of the Q2a, Q2b, CP, D1 and D2 cold masses. Cryogenic and technical service modules are subsequently assembled onto the standard sections. The service module, which is location dependent, may contain the jumper to the cryogenic distribution line with various pipe configurations, phase separation volumes for the saturated 1.9 K helium heat exchangers, piping return loops or distribution manifolds, the beam position monitor (BPM) [9] with its coaxial cables, current leads, the beam screen cooling piping and the beam line cold to warm transitions. Despite a long catalogue of service modules, many components could still be standardised to streamline fabrication. Examples are the reinforcements and cradles of the vacuum vessels, flanges, phase separator bodies and many piping subassemblies. Welds and piping layouts are also standardised, essentially for simplification of assembly procedures and keep the need for special tooling to a minimum.

Another convenience of this modular approach is the possibility to cold test all but the CP and D2 in standard section configuration. This allows for a faster preparation of the magnet for cold testing, as well as to assign a magnet with cold test results already available to a specific slot in the machine.

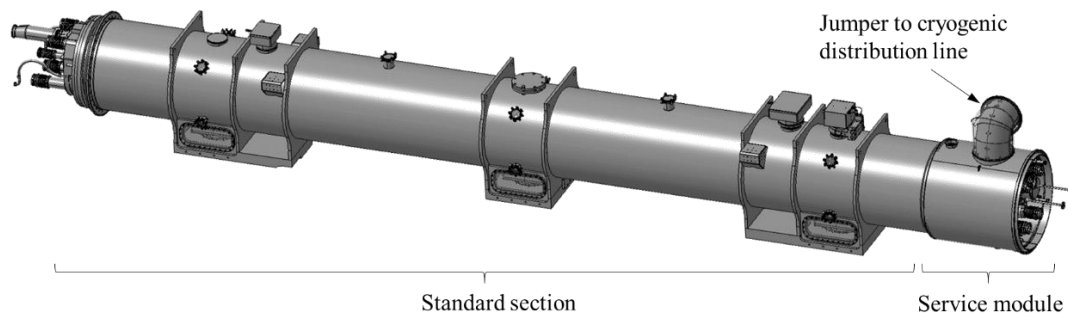


Figure 3. Example of a finished cryostat (Q2b) including the standard section a service module with jumper to the cryogenic line.

5. Main cryostat components

5.1. Cold mass supports

Designing cold mass supports usually requires finding the right balance between thermal and structural performance. This also applies to the HL-LHC supports, however given the compact integration into the cryostat, the design must also include features to allow its assembly with limited accessibility. The first design concept for the support post aimed to solve the assembly difficulties with a two-part column separated by a heat intercept plate [3]. This concept also provided precise temperature control but had structural and manufacturing disadvantages. Stacking parts inevitably results in a cumulation of geometrical deviations and a compromised overall stiffness, ultimately influencing the cold mass alignment inside the cryostat. The final support post design consists of a monolithic glass fibre reinforced epoxy (GFRE) composite column. Instead of a more traditional cylindrical column, a conical shape was adopted since, in this application, it provided better accessibility for bolting to the cold mass, significantly increased lateral stiffness and an overall improvement in stability thanks to a larger diameter base.

Manufacturing can be achieved either by lamination of pre-impregnated glass fibre and curing in an autoclave or by resin transfer moulding (RTM). Given a total of 140 units to be produced, the lamination process came out the most cost effective. Since optimal uniformity of the mechanical and thermal properties is crucial, the maximum void content is specified at 1% of the total volume. The fibre volume fraction is set between 40% and 50%, but more importantly it shall be controlled within a range of two percentage points over the complete production. This ensures the uniformity and repeatability of mechanical and thermal properties, critical for magnet positioning and stability. Machining of the interface flanges and drilling of holes after demoulding allows to obtain precise dimensional tolerances.

The shell thickness, which determines the thermo-mechanical performance of the support, is set at 5.3 mm. This value was obtained through finite element analysis for an imposed Tsai-Wu failure index [10] below 0.5, considering four load cases encompassing loads up to 250 kN in vertical compression and 165 kN in transverse shear.

An externally glued aluminium ring performs as heat intercept at the intermediate temperature range 60 to 80 K, with its position between the cold and warm flanges optimised for minimum exergetic cost. Heat reaching this ring is extracted to the actively cooled thermal shield via flexible straps made from stacks of thin copper sheets.

5.2. Thermal radiation shield

An actively cooled thermal radiation shield is essential in a 1.9 K accelerator magnet cryostat. With a cumulated length of 300 m and a diameter of 0.8 m, aluminium was found to be the most suitable material for this thermal shield. Overall cost is lower when compared to an alternative such as copper, especially since a minimum thickness is needed to keep self-weight deflection low enough. That is because the overall deviation from nominal shape of the shield must be controlled within 5 mm so it will not enter into contact with cold pipes or the cold mass.

The final design consists of two extruded pipes, which include reinforcement wings for additional stiffness and better alignment of the cylindrical shells. The shield is cooled with helium gas in the temperature range of 60 to 80 K flowing through two parallel pipes. This not only provides for a uniform azimuthal temperature profile but, thanks to the symmetric cooling, it also minimizes thermal deflections during temperature transients. The extrusions are made from 6063 aluminium alloy, an alloy particularly well suited for this manufacturing process as it provides the best straightness tolerances out of the mill. On the other hand, 1050 alloy sheets of 4 mm thickness are used for the shells for its superior thermal conductivity, especially in the temperature range of interest. Aluminium to stainless steel transitions are welded at the extremities of the extrusions such that industrially available stainless steel flexible hoses can then be employed to connect across the interconnects.

Supporting the thermal shield either on the vacuum vessel or on the cold mass would result in an undesirable heat load. The solution is to support the thermal shield directly over the heat intercept rings

of the cold mass support posts. Since a thermalisation of the supports posts is required anyway, supporting the thermal shield in this way could be achieved at no heat load cost. CNC machined saddles are incorporated in the thermal shield assembly as mechanical support interfaces and to provide locally improved rigidity.

The thermal shield assembly is executed in two stages. Initially with a pre-assembly of the lower half, with the help of an alignment jig and to be completed later, on the cryostat assembly tooling, with the welding of the upper shells over the cold mass. Counter drilling and riveting is used to pre-position the various parts, together with intermittent welding for adequate heat transfer.

5.3. Vacuum vessel

Considering the importance of precise alignment and overall stability of these cryo-magnets, it was specified to avoid hyperstatic support schemes wherever possible. The HL-LHC cryo-magnets are isostatically supported following a classic 3-2-1 mechanical locating principle: the first locating plane is horizontal, defined by the contact points of three vertically adjustable jacks holding the cryo-magnet weight; a second plane is defined by two points thanks to horizontally adjustable mechanisms integrated in two of the three jacks; and a third locating plane is defined by one point, this one longitudinally adjustable either with a mechanism integrated in the third jack or a variable length tie-rod. The tie-rod is required on Q1 and D1 to resist large longitudinal pressure generated end loads, of the order of 130 kN. The longitudinal position of the jacks supporting the weight was optimized together with the vacuum vessel reinforcements so the cold mass sagitta would not unduly reduce the useful beam aperture. From this optimization resulted a deformed cold mass profile within a +/- 100 μm envelope, achieved thanks to finite element modeling of the cold mass standing on its support posts together with the vacuum vessel. D2 is an exception to the isostatic support goal where its longer cold mass, requires an additional floor jack at its mid-length.

A specific vacuum vessel variant is required for each cold mass type, but they all share a common design. It consists of a cylinder in low carbon fine grain steel, reinforced with rings at the cold mass support points and with machined cradle plates to interface with the GFRE support posts. Steel P355NL2 was chosen as a material specified for pressure applications and, most importantly, with tested resilience down to -50 °C. Such resilience at low temperature is relevant should an accidental leak occur when the magnets are cold.

A moveable flange at one end allows the interconnect bellows to be slid back over the vacuum vessel to allow in-situ access to the piping and busbars between magnets. Both this flange and the one at the opposite end, are machined from 304L stainless steel forged rings. Side ports provide access for assembly and inspection of the cold mass supports.

Each fully welded vessel is subjected to a vibratory stress relieving process. Finish machining is then performed to obtain precise and stable interfaces for the cold mass supports. Figure 4 shows the first vacuum vessels units at CERN and ready for further assembly. The possibility of stacking vessels for storage was considered in the design of the reinforcements.



Figure 4. First production batch of vacuum vessels.

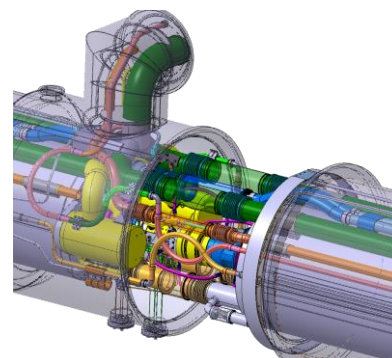


Figure 5. Example of interconnect between cryo-magnets.

5.4. Interconnects and expansion joints

Cryogenic lines between adjacent cryo-magnets require flexible elements to accommodate thermal contraction. These elements must also provide transverse flexibility to permit offsets at installation and relative movements during alignment of the magnets. Corrugated metal bellows in 316L stainless steel are used in all lines above 40 mm inner diameter. They are assembled in a universal expansion joint configuration, i.e. two bellows with a pipe section between them, thus minimizing the transverse stiffness through the lever arm effect created by the intermediate pipe. Buckling is a critical design aspect for expansion joints that must accommodate long axial strokes under high pressure. This is our case, as axial strokes reach 34 mm with pressures in the range of 5 to 25 bar. The design was conducted according to EN 14917 and complemented with finite element analysis to independently validate the results for the buckling failure modes. Flexible hoses are specified for pipes with diameters lower than 40 mm.

5.5. Cryogenic and technical service modules

Grouping the cryogenic piping in a dedicated service module presents an integration advantage since this module can be made with a diameter larger than the standard section cylinder. This is possible because the full cold mass weight and transverse loads are carried in the standard section vacuum vessel, thus avoiding the need for reinforcement ribs around the service module. It is thanks to this locally enlarged diameter (1018 mm) that integration of all services became possible inside the cryostat. As shown in figure 6, integration remains very compact nevertheless, especially where helium phase separation volumes and jumper piping are required.

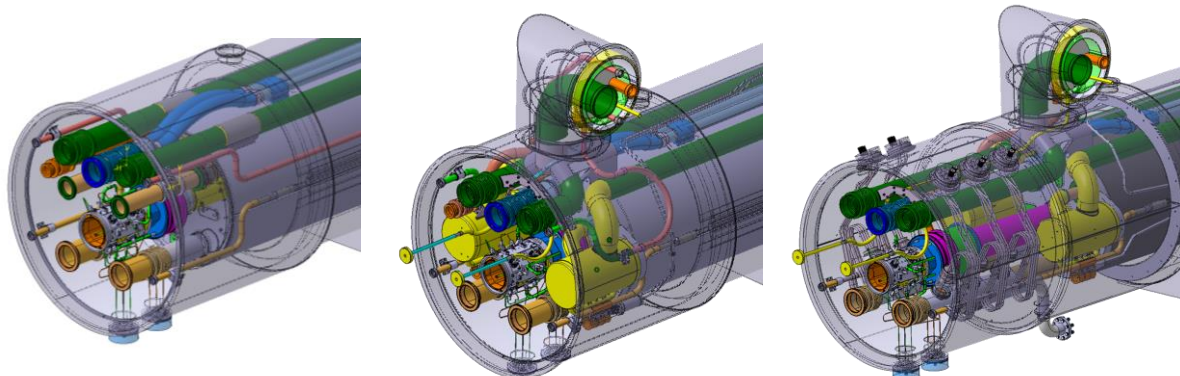


Figure 6. Views of three examples of service module: the simplest configuration (Q3) in the left picture; a version with phase separators, pumping lines and jumper (Q2b) in the middle; and on the right a version for CP including the current lead module.

The helium phase separator subassemblies, made from 316L stainless steel, exist in two versions depending on the tunnel slope at the place of installation since they must connect either to the cold mass on which they are mounted, or to the neighbouring cold mass through the interconnect piping. Due to the tight space constraints, they feature rather intricate pipe connections that must be manufactured and leak-tested prior to assembly in the cryostat. Both phase separator and jumper piping are mounted to the cold mass extremity on welded stainless steel supports. The routing of lines inside the service module was thoroughly optimised such that enough clearance volume around each pipe is available for welding and eventual repairs requiring installation of pipe cutting machines.

An aluminium thermal shield extension is welded to and thermalized from the standard section thermal shield. The service module assembly is completed with its vacuum vessel, made from 6 mm thick 304L stainless steel and welded to the standard section end flange. Beam vacuum components such as the beam screen and the beam position monitor are installed at the end of the assembly process since their cleanliness is critical.

The CP cryostat comprises an additional module specifically designed for the integration of conduction cooled current leads, used to locally power the high order correctors.

6. Assembly and special tooling

Handling the cold masses and inserting them into the vacuum vessels can only be done horizontally where cold mass deformation must be minimized so as to not overstrain the coils. The tooling developed for this assembly uses temporary rails extending into the vacuum vessel, over which the cold mass slides while standing on sledges equipped with plain bearings in a low friction material (Figure 7). The cold mass insertion or removal is achieved with the help of a winch pulling directly on the sledges. Integrated lifting jacks are used to raise the cold mass and allow extraction of the temporary rails. The cold mass insertion process is completed with the assembly of the cold mass support posts from underneath the vessel, after which the cold mass is lowered and the load transferred from the tooling jacks to the vacuum vessel.

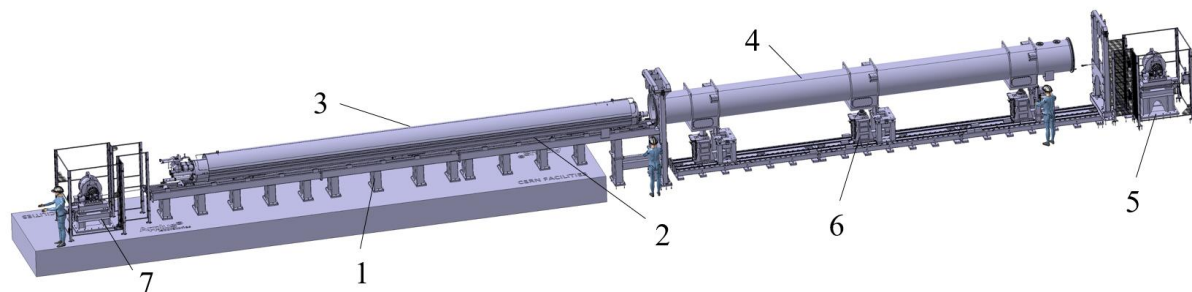


Figure 7. Overview of the cold mass assembly tooling. An assembly table (1) equipped with rails (2) is used to prepare the cold mass and thermal shield (3). The cold mass slides over the rails as it is pulled into the vacuum vessel (4) by a forward winch (5). Jacks (6) lift the cold mass for extraction of the rails from the vacuum vessel. If needed (e.g. for magnet repair) a rearward winch (7) allows to pull the cold mass out of the vacuum vessel.

Metrological inspection of the cold mass straightness and alignment with respect to the vacuum vessel is subsequently performed with a laser tracker. Should an out of tolerance deviation be found, it is possible to readjust the cold mass supports vertically with shims and horizontally with adjustable base plates at the sliding supports.

The cryo-magnet is then removed from this tooling and completed with its instrumentation feedthroughs in preparation for cold testing. Various welding stations equipped with jigs to locate pipes during welding ensure the precise and correct positioning of each cryo-magnet interface during assembly of the service module piping.

7. Conclusion

The cryostat design presented in this paper was inspired from the positive return of experience from over a decade of operation of the LHC, while adding many new features to accommodate the demanding HL-LHC requirements. A larger cold mass diameter and several cryogenic and busbar lines were integrated into a cryostat that is nevertheless still compatible with the transport constraints within the existing machine tunnel. Precise magnet positioning and stability relies on GFRE cold mass support posts with a conical shape that has both the advantage of increased structural strength, to withstand pressure induced loads, and of remarkably higher stiffness. Overall static heat load is minimized, due again to the support post design and to the actively cooled thermal shield, which is attached directly onto the heat intercept of the support posts. High pressure loads and weight are safely resisted without compromising alignment through the adoption of an isostatic cryo-magnet support scheme. The optimised vacuum vessel structural design ensures minimal cold mass sagitta as to not impair useful beam aperture. Interconnects have been developed around the concept of universal expansion joints to

give enough flexibility for both thermal contraction and transverse offsets between cold masses. All these features, in combination with a modular approach for component fabrication and assembly made it possible to achieve a final cryostat design complying with the challenging requirements of the HL-LHC under controlled cost.

At the time of writing the main components have been released for fabrication and the tooling installed and commissioned. The assembly of the first cryo-magnets is due to start in the coming months.

8. References

- [1] Aberle O et al 2020 High-Luminosity Large Hadron Collider (HL-LHC): Technical design report *CERN CERN-2020-010*
- [2] Todesco E et al 2021 The High Luminosity LHC interaction region magnets towards series production *Superconductor Science and Technology* Vol 34 053001
- [3] Ramos D et al 2017 Conceptual design of the cryostat for the new high luminosity (HL-LHC) triplet magnets *IOP Conference Series: Materials Science and Engineering* Vol 278 012175
- [4] Bozza G et al 2015 FP7 High Luminosity Large Hadron Collider Design Study - Design Study of the Cooling *CERN CERN-ACC-2015-0125*
- [5] Rousset B et al 2019 Superfluid Helium Cooling and Compact Heat Exchanger for HL-LHC D2 Recombination Dipoles *IOP Conference Series: Materials Science and Engineering* Vol 502 012114
- [6] Poncet A et al 2009 Final Design and Experimental Validation of the Thermal Performance of the LHC Lattice Cryostats *Advances in Cryogenic Engineering* Vol 49-A 487-493
- [7] Mainaud Durand H et al 2018 Frequency Scanning Interferometry as New Solution for On-line Monitoring Inside a Cryostat for the HL-LHC project *Proc. IPAC'18 Vancouver* pp. 1986-1989 WEPAF068
- [8] Padeloup F et al 2020 Thermo-Electric Design of the Protection and Diagnostic Feeders of the HL-LHC Triplets *IOP Conference Series: Materials Science and Engineering* 755 012128
- [9] Krupa M 2019 Beam Instrumentation and Diagnostics for High Luminosity LHC *Proc. IBIC'19 Malmö* pp. 1-8
- [10] Tsai S W and Wu E M 1971 A General Theory of Strength for Anisotropic Materials *Journal of Composite Materials* Vol 5 pp 58-80

Acknowledgments

This work was only possible thanks to the contribution of many colleagues from CERN, collaborating institutes and contractors involved in the project. We wish to especially thank all technicians and draftsmen that contributed with their experience and dedication to materialise numerous concepts implemented in this design.